



# [1.1]Diborataferrocenophane: A Highly Efficient Li<sup>+</sup> Scavenger\*\*

Matthias Scheibitz, Rainer F. Winter, Michael Bolte, Hans-Wolfram Lerner, and Matthias Wagner\*

- Dapprich, J. M. Millam, A. D. Daniels, K. N. Kudin, M. C. Strain, O. Farkas, J. Tomasi, V. Barone, M. Cossi, R. Cammi, B. Mennucci, C. Pomelli, C. Adamo, S. Clifford, J. Ochterski, G. A. Petersson, P. Y. Ayala, Q. Cui, K. Morokuma, D. K. Malick, A. D. Rabuck, K. Raghavachari, J. B. Foresman, J. Cioslowski, J. V. Ortiz, B. B. Stefanov, G. Liu, A. Liashenko, P. Piskorz, I. Komaromi, R. Gomperts, R. L. Martin, D. J. Fox, T. Keith, M. A. Al-Laham, C. Y. Peng, A. Nanayakkara, C. Gonzalez, M. Challacombe, P. M. W. Gill, B. G. Johnson, W. Chen, M. W. Wong, J. L. Andres, M. Head-Gordon, E. S. Replogle, J. A. Pople, Gaussian, Inc., Pittsburgh, PA, **1998**.
- [10] D. Wittenberg, H. A. McNince, H. Gilman, *J. Am. Chem. Soc.* **1958**, *80*, 5418–5422.
- [11] For examples, see M. S. Newman, *Effects in Organic Chemistry*, Wiley, New York, **1956**; L. N. Ferguson, *The Modern Structural Theory of Organic Chemistry*, Prentice-Hall, Englewood Cliffs, NJ, **1963**.
- [12] a) M. Beller, *Angew. Chem.* **1995**, *107*, 1436–1437; *Angew. Chem. Int. Ed. Engl.* **1995**, *34*, 1316; b) J. F. Hartwig, *Synlett* **1997**, 329; c) J. F. Hartwig, *Angew. Chem.* **1998**, *110*, 2154–2177; *Angew. Chem. Int. Ed.* **1998**, *37*, 2046–2067; d) J. P. Wolfe, S. Wagaw, J.-F. Marcoux, S. L. Buchwald, *Acc. Chem. Res.* **1998**, *31*, 805; e) J. F. Hartwig, *Acc. Chem. Res.* **1998**, *31*, 852.
- [13] Physical data for **1**: White solid; <sup>1</sup>H NMR (400 MHz, CDCl<sub>3</sub>): δ = 7.30 (d, 4H), 7.17 (d, 4H), 6.90 (d, 4H), 6.75 (dd, 4H), 6.47 (d, 4H), 3.94 (s, 6H), 3.64 ppm (s, 12H); <sup>13</sup>C NMR (75 MHz, CDCl<sub>3</sub>): δ = 158.9, 152.5, 145.2, 136.83, 132.30, 119.5, 118.0, 117.3, 116.8, 116.1, 55.5 ppm; <sup>13</sup>C NMR (75 MHz, C<sub>6</sub>D<sub>6</sub>): δ = 159.4, 153.7, 146.0, 137.5, 132.8, 119.3, 119.0, 118.7, 117.6, 116.4, 55.0, 54.9 ppm; elemental analysis (%): calcd for C<sub>42</sub>H<sub>38</sub>N<sub>2</sub>O<sub>6</sub>Si: C 72.60, H 5.51, N 4.03; found: C 72.41, H 5.44, N 3.97.
- [14] The oxidation potential of trianisylamine was 0.16 V vs Fc/Fc<sup>+</sup> under the same conditions. This discrepancy of the first oxidation potential between **1** and trianisylamine probably results from a difference in conformation of the trianisylamine moieties. In **1**, the propellerlike conformation can be hardly adopted because of its spiro structure.
- [15] Compound **1** (69 mg, 0.1 mmol) was dissolved in dry dichloromethane and stirred at –78 °C under argon. SbCl<sub>5</sub> (0.5 ml, 1 M in CH<sub>2</sub>Cl<sub>2</sub>) was added to the solution. After 10 min, the resulting blue solution was poured into dry diethyl ether. The precipitate was washed with dry diethyl ether to provide **1**(SbCl<sub>6</sub>)<sub>2</sub> (110 mg, 81 %) as a greenish blue solid. **1**(SbCl<sub>6</sub>)<sub>2</sub>: elemental analysis (%): calcd for C<sub>42</sub>H<sub>38</sub>Cl<sub>12</sub>N<sub>2</sub>O<sub>6</sub>Sb<sub>2</sub>Si: C 36.99, H 2.81, N 2.05, Cl 31.19; found: C 36.99, H 2.71, N 2.05, Cl 29.61.
- [16] The isolated solid sample was dissolved in CH<sub>2</sub>Cl<sub>2</sub>, and the ESR signal intensity was compared to that of a sample oxidized in situ at the same concentration. The two signals gave the same fine structure with almost the same intensity.
- [17] Example of oxidation with SbCl<sub>5</sub> in CH<sub>2</sub>Cl<sub>2</sub>: H. Bock, A. Rauschenbach, K. Ruppert, Z. Havlas, *Angew. Chem.* **1991**, *103*, 706–708; *Angew. Chem. Int. Ed.* **1998**, *37*, 714–716.
- [18] N. Hirota, *J. Am. Chem. Soc.* **1967**, *89*, 32–41.
- [19] K. Mukai, A. Sogabe, *J. Chem. Phys.* **1980**, *72*, 598–601.
- [20] B. Bleaney, K. D. Bowers, *Proc. R. Soc. London Ser. A* **1952**, *214*, 451–456.

In various cases, electrophilic substitution reactions of ferrocene are known to proceed via precomplexation of the iron atom by the electrophile.<sup>[1]</sup> Moreover, direct iron-to-metal bonding appears to influence the complexation behavior of certain ferrocene-based redox-switchable cryptands,<sup>[2]</sup> as well as the properties of catalytically active 2-metalla[3]-ferrocenophanes (metal = Ti<sup>IV</sup>, Pd<sup>II</sup>, Pt<sup>II</sup>).<sup>[3]</sup> The interaction of ferrocene with Li<sup>+</sup> was studied theoretically by Ugalde et al.,<sup>[4]</sup> who located two minima on the energy surface. In the lower energy structure, the lithium cation is η<sup>5</sup>-coordinated on top of one of the cyclopentadienyl rings (**I**; Scheme 1). The second minimum structure **II** is 8 kcal mol<sup>–1</sup> higher in energy and has the Li<sup>+</sup> ion bonded laterally to the iron atom. We recently reported the synthesis and structural characterization of a ferrocene/gallium(i) cation complex with essentially the same structural motif as **I**.<sup>[5]</sup> Here we report on the isolation of a ferrocene/lithium complex that provides experimental evidence for the existence of structure **II**.

When a slurry of 1,1'-dilithioferrocene (**1**)<sup>[6]</sup> in hexane is treated with a solution of 1,1'-bis(dimethylboryl)ferrocene (**2**) in THF,<sup>[7]</sup> the cyclic dinuclear aggregate **3**<sup>2–</sup> is formed in good yield (Scheme 1). X-ray quality crystals of [3-Li]Li([12]crown-4)<sub>2</sub> were grown by gas-phase diffusion of diethyl ether into a solution of the crude material in THF after addition of [12]crown-4.

The <sup>11</sup>B NMR spectrum of [3-Li]Li([12]crown-4)<sub>2</sub> reveals one signal at δ(<sup>11</sup>B, [D<sub>8</sub>]THF) = –21.8 ppm, which testifies to

[\*] Prof. Dr. M. Wagner, Dipl.-Chem. M. Scheibitz, Dr. H.-W. Lerner  
Institut für Anorganische Chemie  
Johann Wolfgang Goethe-Universität Frankfurt  
Marie-Curie-Strasse 11, 60439 Frankfurt/Main (Germany)  
Fax: (+49) 69-798-29260  
E-mail: matthias.wagner@chemie.uni-frankfurt.de

Dr. R. F. Winter  
Institut für Anorganische Chemie  
Universität Stuttgart  
Pfaffenwaldring 55, 70569 Stuttgart (Germany)

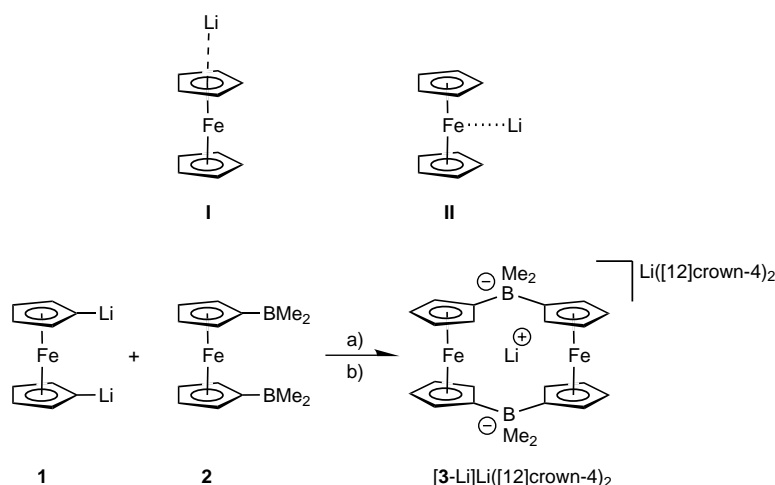
Dr. M. Bolte  
Institut für Organische Chemie  
Johann Wolfgang Goethe-Universität Frankfurt  
Marie-Curie-Strasse 11, 60439 Frankfurt/Main (Germany)

[\*] X-ray crystallography

[\*\*] We wish to thank Prof. Dr. M. U. Schmidt (Universität Frankfurt) for helpful discussions. M.W. is grateful to the Deutsche Forschungsgemeinschaft (DFG) for financial support. M.S. wishes to thank the Fonds der Chemischen Industrie (FCI) and the Bundesministerium für Bildung und Forschung (BMBF) for a PhD grant. R.W. acknowledges support by the Stiftung Volkswagenwerk.



Supporting information for this article is available on the WWW under <http://www.angewandte.org> or from the author.



**Scheme 1.** a) THF/hexane, RT; b) excess [12]crown-4, RT.

the presence of tetracoordinate boron atoms.<sup>[8]</sup> In the  $^1\text{H}$  NMR spectrum, only one signal is observed for all four methyl groups ( $\delta(^1\text{H}, [\text{D}_8]\text{THF}) = -0.25$  ppm). The signal is broad and has a doublet line shape due to partially resolved  $^2J(\text{B}, \text{H})$  coupling. The cyclopentadienyl rings give rise to two well-resolved pseudotriplets at  $\delta(^1\text{H}, [\text{D}_8]\text{THF}) = 3.86$  and  $3.99$  ppm; the corresponding carbon resonances appear at  $\delta(^{13}\text{C}, [\text{D}_8]\text{THF}) = 69.8$  and  $74.0$  ppm. Both the  $^1\text{H}$  and the  $^{13}\text{C}$  NMR patterns indicate a high average symmetry of the molecule in solution. This observation can be explained by a degenerate *syn-syn* isomerization of the [1.1]ferrocenophane framework, which leads to fast exchange of the methyl groups in the *exo* and *endo* positions of the  $\text{BMe}_2$  bridges (the *anti* conformation of [1.1]ferrocenophanes with small bridging atoms is disfavored for steric reasons).<sup>[9]</sup>

Most interestingly, the  $^7\text{Li}$  NMR spectrum displays two signals at  $\delta(^7\text{Li}, [\text{D}_8]\text{THF}) = -0.19$  and  $4.29$  ppm with an integral ratio of 1:1. Comparison with the spectra of  $\text{LiCl}$  ( $\delta(^7\text{Li}, [\text{D}_8]\text{THF}) = 0.30$  ppm) and  $\text{Li}([12]\text{crown-4})_2\text{Cl}$  ( $\delta(^7\text{Li}, [\text{D}_8]\text{THF}) = -0.21$  ppm) clearly shows that the signal at higher field must be assigned to a  $[\text{Li}([12]\text{crown-4})_2]^+$  cation. The signal at  $4.29$  ppm obviously corresponds to the second lithium cation, which appears to be surrounded by a distinctly different ligand sphere. At ambient temperature, any exchange of  $\text{Li}^+$  between the two coordination sites is clearly slow on the NMR timescale. The  $^7\text{Li}$  NMR spectrum does not change when more [12]crown-4 is added to the NMR tube.

The structure of  $[\text{3-Li}]\text{Li}([12]\text{crown-4})_2$  in the solid state was finally established by X-ray crystallography (Figure 1).<sup>[10]</sup> The molecule contains a [1.1]ferrocenophane ring in a twisted *syn* conformation (dihedral angles:  $\text{C1-C5}/\text{C31-C35}$   $21.3^\circ$ ;  $\text{C11-C15}/\text{C21-C25}$   $23.1^\circ$ ).<sup>[11]</sup> In agreement with the NMR data, one of the lithium cations is coordinated by two crown ether molecules and forms the well-known complex  $[\text{Li}([12]\text{crown-4})_2]^+$ . The second lithium cation is located inside the ferrocenophane cavity, most likely trapped by the electrostatic field originating from the two anionic dimethylborate bridges ( $\text{Li1}\cdots\text{B1}$   $2.314(6)$ ,  $\text{Li1}\cdots\text{B2}$   $2.309(6)$  Å;  $\text{B1}\cdots\text{Li1}\cdots\text{B2}$   $179.2(3)^\circ$ ;  $\text{Li1}$  is not located on a special position). The

distances between the  $\text{Li}^+$  ion and the iron centers are somewhat larger than the value calculated for structure **II** (**II**:  $\text{Li}\cdots\text{Fe}$   $2.4$  Å;  $[\text{3-Li}]^-$ :  $\text{Li1}\cdots\text{Fe1}$   $2.720(6)$ ,  $\text{Li1}\cdots\text{Fe2}$   $2.706(5)$  Å;  $\text{Fe1}\cdots\text{Li1}\cdots\text{Fe2}$   $128.2(2)^\circ$ ). As was predicted by Ugalde et al.,<sup>[4]</sup> the close vicinity of the  $\text{Li}^+$  ion does not lead to a major distortion of the ferrocene structure ( $\text{COG-Fe1-COG}'$   $175.6^\circ$ ,  $\text{COG-Fe2-COG}'$   $174.9^\circ$ ; COG: center of gravity of a  $\text{C}_5\text{H}_4$  ring). We observe only little bending of the boron centers out of the planes of the attached Cp rings (av  $\text{COG-C(ipso)-B}$   $167.3(3)^\circ$ ), and the distances between the carbon atoms C1, C11, C21, C31 and the  $\text{Li}^+$  ion are rather large (av  $\text{C(ipso)}\cdots\text{Li1}$   $2.361(5)$  Å). These findings suggest that there is no substantial degree of charge transfer from the Cp rings to the lithium cation. The question thus arises whether the function of the diborylated ferrocenophane is adequately described as merely

providing an anionic macrocycle in which  $\text{Li}^+$  is trapped.  $[\text{3-Li}]^-$  containing a naked lithium cation in close proximity to a ferrocene moiety represents a reasonable approximation of **II**, as it was predicted to exist under gas-phase conditions. Ugalde et al. calculated the lithium cation basicity (LCB) of ferrocene at  $T = 298$  K for structure **II** and obtained a value of  $29.4$  kcal mol $^{-1}$ ,<sup>[4]</sup> which, in comparison with other LCB data determined both theoretically and experimentally by Burk et al.,<sup>[12]</sup> leads to the conclusion that ferrocene behaves as a moderately strong base toward the lithium cation. Since  $[\text{3-Li}]^-$  has two ferrocene moieties which, in addition, are much more electron-rich than ferrocene itself (see below and also ref. [13]), a contribution from bonding  $\text{Fe}\cdots\text{Li}$  interactions to the stability of the aggregate should be considered.

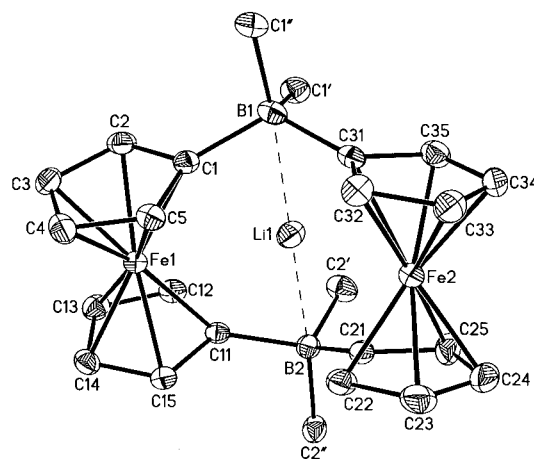


**Figure 1.** Molecular structure and numbering scheme of  $[\text{3-Li}]\text{Li}([12]\text{crown-4})_2$  (thermal ellipsoids shown at the 50% probability level,  $\text{Li}([12]\text{crown-4})_2^+$  fragment and hydrogen atoms omitted for clarity). Selected atom-atom distances [Å], bond lengths [Å], angles [°], and torsion angles [°]:  $\text{B1-C1}$   $1.651(5)$ ,  $\text{B1-C31}$   $1.651(5)$ ,  $\text{B2-C11}$   $1.646(5)$ ,  $\text{B2-C21}$   $1.659(5)$ ,  $\text{Li1}\cdots\text{B1}$   $2.314(6)$ ,  $\text{Li1}\cdots\text{B2}$   $2.309(6)$ ,  $\text{Li1}\cdots\text{Fe1}$   $2.720(6)$ ,  $\text{Li1}\cdots\text{Fe2}$   $2.706(5)$ ,  $\text{C1-B1-C31}$   $115.7(3)$ ,  $\text{C11-B2-C21}$   $114.8(3)$ ,  $\text{B1}\cdots\text{Li1}\cdots\text{B2}$   $179.2(3)$ ,  $\text{Fe1}\cdots\text{Li1}\cdots\text{Fe2}$   $128.2(2)$ ,  $\text{C2-C1-B1-C1}'$   $-38.9(4)$ ,  $\text{C2-C1-B1-C1}''$   $78.1(3)$ ,  $\text{C25-C21-B2-C2}'$   $-38.7(4)$ ,  $\text{C25-C21-B2-C2}''$   $78.5(4)$ .

In cyclic voltammetry experiments ( $\text{CH}_2\text{Cl}_2$ , 0.2 M  $\text{NBu}_4\text{PF}_6$ )  $[\mathbf{3}\text{-Li}]\text{Li}([\mathbf{12}]\text{crown-4})_2$  was irreversibly oxidized at a peak potential of  $-0.58\text{ V}$  (vs  $\text{FcH}/\text{FcH}^+$ ,  $v=0.1\text{ V s}^{-1}$ ; Figure 2a).<sup>[14]</sup> This sizable cathodic shift with respect to ferrocene reflects the high electron density in the anionic  $[\mathbf{1.1}]\text{ferrocenophane}$ .<sup>[15]</sup> When, after oxidation, the sweep is continued into the cathodic regime, two partially reversible waves emerge at even more negative half-wave potentials

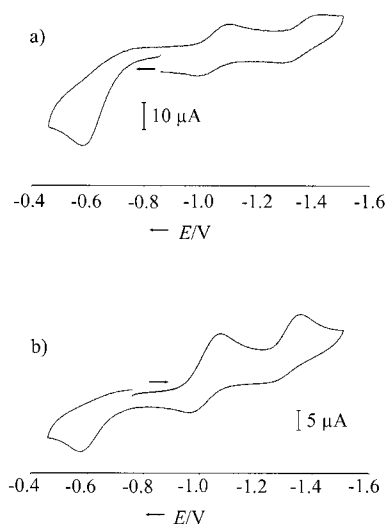


**Figure 2.** a) Cyclic voltammogram of  $[\mathbf{3}\text{-Li}]\text{Li}([\mathbf{12}]\text{crown-4})_2$  ( $\text{CH}_2\text{Cl}_2$ , 0.2 M  $\text{NBu}_4\text{PF}_6$ ,  $v=0.1\text{ V s}^{-1}$ , vs  $\text{FcH}/\text{FcH}^+$ ); b) Cyclic voltammogram of  $[\mathbf{3}\text{-Li}]\text{Li}([\mathbf{12}]\text{crown-4})_2$  after exhaustive oxidation ( $\text{CH}_2\text{Cl}_2$ , 0.2 M  $\text{NBu}_4\text{PF}_6$ ,  $v=0.1\text{ V s}^{-1}$ , vs  $\text{FcH}/\text{FcH}^+$ ).

( $E_{1/2} = -1.02, -1.33\text{ V}$ ;  $\Delta E_p = 84$  and  $111\text{ mV}$ , respectively).<sup>[16]</sup> These waves are not observed if the cathodic scan is performed first and are thus assigned to electroactive product(s) arising from a chemical step following oxidation. On bulk electrolysis at  $-0.38\text{ V}$  the electroactive product(s) mentioned above were cleanly produced. Voltammetric scans after electrolysis reveal both cathodic waves to be only partially reversible, and this again indicates a chemical process following electron transfer. If after the cathodic scan the sweep is taken back into the more anodic regime, the oxidation wave of the parent  $[\mathbf{3}\text{-Li}]\text{Li}([\mathbf{12}]\text{crown-4})_2$  reappears (Figure 2b). In accordance with the voltammetric data, bulk reduction at  $-1.20\text{ V}$  gives back the starting material as the principal product. We conclude that the oxidation/reduction sequence constitutes an overall chemically reversible cycle connected by irreversible individual steps. Considering the pronounced cathodic shift of both reduction potentials relative to the oxidation potential of parent  $[\mathbf{3}\text{-Li}]^-$ , a plausible scenario is that upon oxidation of  $[\mathbf{3}\text{-Li}]^-$  the encapsulated  $\text{Li}^+$  ion is expelled from the macrocycle.

$[\mathbf{3}]^{2-}$  is a novel type of redox-switchable lithium scavenger. Contrary to other functionally related complexes,<sup>[17]</sup> the lithium ion in  $[\mathbf{3}\text{-Li}]^-$  is not coordinated by main-group Lewis bases. We therefore suggest that  $[\mathbf{3}\text{-Li}]\text{Li}([\mathbf{12}]\text{crown-4})_2$  could be used as an easily accessible model system to study the interaction of ferrocene with the unperturbed naked lithium cation.

## Experimental Section

**$[\mathbf{3}\text{-Li}]\text{Li}([\mathbf{12}]\text{crown-4})_2$ :** A solution of **2** (0.29 g, 1.09 mmol) in THF (5 mL) was added to a slurry of **1**·2 tmeda (0.47 g, 1.09 mmol; tmeda = *N,N,N',N'*-tetramethylethylenediamine) in hexane (20 mL) with stirring at ambient temperature. The reaction mixture was stirred for 2 h. After filtration, the remaining solid was triturated in hexane ( $2 \times 10\text{ mL}$ ) and dried in vacuo. A solution of the crude product in THF was treated with  $[\mathbf{12}]\text{crown-4}$  (0.37 g, 2.20 mmol) and then slowly layered with diethyl ether by gas-phase diffusion to yield X-ray quality crystals of  $[\mathbf{3}\text{-Li}]\text{Li}([\mathbf{12}]\text{crown-4})_2$ . Yield: 0.39 g (44 %).

$^{11}\text{B}$  NMR (128.4 MHz,  $[\text{D}_8]\text{THF}$ ):  $\delta = -21.8\text{ ppm}$  ( $h_{1/2} = 20\text{ Hz}$ );  $^7\text{Li}$  NMR (155.5 MHz,  $[\text{D}_8]\text{THF}$ ):  $\delta = -0.19$  ( $[\text{Li}([\mathbf{12}]\text{crown-4})_2]^+$ ), 4.29 ppm ( $[\mathbf{3}\text{-Li}]^-$ );  $^1\text{H}$  NMR (250.1 MHz,  $[\text{D}_8]\text{THF}$ ):  $\delta = -0.25$  (br, 12H;  $\text{CH}_3$ ), 3.61 (s, 32H;  $\text{CH}_2$ ), 3.86, 3.99 ppm ( $2 \times t$ ,  $2 \times 8\text{ H}$ ,  $^3J(\text{H,H}) = ^4J(\text{H,H}) = 1.7\text{ Hz}$ ;  $\text{C}_5\text{H}_4$ );  $^{13}\text{C}$  NMR (62.9 MHz,  $[\text{D}_8]\text{THF}$ ):  $\delta$  = not observed ( $\text{CH}_3$ ), 69.8 ( $\text{C}_5\text{H}_4$ ), 72.0 ( $\text{CH}_2$ ), 74.0 ppm ( $\text{C}_5\text{H}_4$ ), not observed ( $\text{C}_5\text{H}_4\text{-ipso}$ ).  $^{11}\text{B}$  and  $^7\text{Li}$  NMR spectra are reported relative to external  $\text{BF}_3\cdot\text{Et}_2\text{O}$  and  $\text{LiCl}/\text{D}_2\text{O}$ , respectively. Elemental analysis (%) calcd for  $\text{C}_{40}\text{H}_{60}\text{B}_2\text{Fe}_2\text{Li}_2\text{O}_8$  (816.08): C 58.87, H 7.41; found: C 58.55, H 7.51.

Received: July 17, 2002

Revised: November 20, 2002 [Z19759]

- [1] M. J. Mayor-López, J. Weber, B. Mannfors, A. F. Cunningham, Jr., *Organometallics* **1998**, *17*, 4983–4991.
- [2] J. C. Medina, T. T. Goodnow, M. T. Rojas, J. L. Atwood, B. C. Lynn, A. E. Kaifer, G. W. Gokel, *J. Am. Chem. Soc.* **1992**, *114*, 10583–10595.
- [3] M. Herberhold, *Angew. Chem.* **2002**, *114*, 998–1000; *Angew. Chem. Int. Ed.* **2002**, *41*, 956–958.
- [4] A. Irigoras, J. M. Mercero, I. Silanes, J. M. Ugalde, *J. Am. Chem. Soc.* **2001**, *123*, 5040–5043.
- [5] S. Scholz, J. C. Green, H.-W. Lerner, M. Bolte, M. Wagner, *Chem. Commun.* **2002**, 36–37.
- [6] M. D. Rausch, D. J. Ciappenelli, *J. Organomet. Chem.* **1967**, *10*, 127–136.
- [7] W. Ruf, T. Renk, W. Siebert, *Z. Naturforsch. B* **1976**, *31*, 1028–1034.
- [8] “Nuclear Magnetic Resonance Spectroscopy of Boron Compounds”: H. Nöth, B. Wrackmeyer in *NMR Basic Principles and Progress*, Vol. 14 (Eds.: P. Diehl, E. Fluck, R. Kosfeld), Springer, Berlin, **1978**.
- [9] U. T. Mueller-Westerhoff, *Angew. Chem.* **1986**, *98*, 700–716; *Angew. Chem. Int. Ed. Engl.* **1986**, *25*, 702–717.
- [10] X-ray crystal structure analysis of  $[\mathbf{3}\text{-Li}]\text{Li}([\mathbf{12}]\text{crown-4})_2$ : STOE-IPDS-II two-circle diffractometer,  $\text{MoK}_\alpha$  radiation ( $\lambda = 0.71073\text{ Å}$ ),  $\omega$  scans, empirical absorption correction, the structure was solved by direct methods using SHELXS-97 and refined with SHELXL-97 (G. M. Sheldrick, Universität Göttingen, Germany, **1997**) by full-matrix least-squares methods against  $F^2$ . Hydrogen atoms were placed on ideal positions and refined with fixed isotropic displacement parameters using a riding model. In addition, the torsion angles about the B–CH<sub>3</sub> bonds were refined.  $[\text{C}_{24}\text{H}_{28}\text{B}_2\text{Fe}_2\text{Li}]^+[(\text{C}_8\text{O}_4\text{H}_{16})_2\text{Li}]^-$ ,  $M_r = 816.08\text{ g mol}^{-1}$ , crystal dimensions  $0.62 \times 0.16 \times 0.14\text{ mm}$ , pale yellow needle, triclinic, space group  $P\bar{1}$ ;  $a = 10.519(1)$ ,  $b = 13.643(1)$ ,  $c = 14.986(2)\text{ Å}$ ,  $\alpha = 69.208(8)$ ,  $\beta = 88.794(8)$ ,  $\gamma = 81.104(8)^\circ$ ,  $V = 1985.1(4)\text{ Å}^3$ ,  $Z = 2$ ;  $\rho_{\text{calcd}} = 1.365\text{ g cm}^{-3}$ ;  $\mu = 0.781\text{ mm}^{-1}$ , min./max. transmission  $0.643/0.8985$ ;  $2\theta_{\text{max}} = 50.7^\circ$ ;  $T = 100(2)\text{ K}$ ; of 25 706 measured reflections, 6953 were independent ( $R_{\text{int}} = 0.0826$ ); 489 parameters refined;  $R1 = 0.070$  (all data),  $wR2 = 0.1048$  (all data);  $S = 1.019$ , min./max. residual electron density  $-0.597/0.337\text{ e Å}^{-3}$ . CCDC-189707 contains the supplementary crystallographic data for this paper. These data can be obtained free of charge via [www.ccdc.cam.ac.uk/conts/](http://www.ccdc.cam.ac.uk/conts/)

retrieving.html (or from the Cambridge Crystallographic Data Centre, 12, Union Road, Cambridge CB21EZ, UK; fax: (+44) 1223-336-033; or deposit@ccdc.cam.ac.uk).

- [11] For crystal structures of a) [1.1]disila-, b) [1.1]distanna-, c) [1.1]diplumba-, and d) [1.1]digallaferrocenophanes, see a) D. L. Zechel, D. A. Foucher, J. K. Pudelski, G. P. A. Yap, A. L. Rheingold, I. Manners, *J. Chem. Soc. Dalton Trans.* **1995**, 1893–1899; b) A. Clearfield, C. J. Simmons, H. P. Withers, Jr., D. Seyferth, *Inorg. Chim. Acta* **1983**, 75, 139–144; c) G. Utri, K. E. Schwarzthans, G. M. Allmaier, *Z. Naturforsch. B* **1990**, 45, 755–762; d) W. Uhl, I. Hahn, A. Jantschak, T. Spies, *J. Organomet. Chem.* **2001**, 637–639, 300–303; P. Jutzi, N. Lenze, B. Neumann, H.-G. Stammer, *Angew. Chem.* **2001**, 113, 1470–1473; *Angew. Chem. Int. Ed.* **2001**, 40, 1424–1427.
- [12] P. Burk, I. A. Koppel, I. Koppel, R. Kurg, J.-F. Gal, P.-C. Maria, M. Herreros, R. Notario, J.-L. M. Abboud, F. Anvia, R. W. Taft, *J. Phys. Chem. A* **2000**, 104, 2824–2833.
- [13] M. Fontani, F. Peters, W. Scherer, W. Wachter, M. Wagner, P. Zanello, *Eur. J. Inorg. Chem.* **1998**, 1453–1465; M. Fontani, F. Peters, W. Scherer, W. Wachter, M. Wagner, P. Zanello, *Eur. J. Inorg. Chem.* **1998**, 2087.
- [14] a) The cell for voltammetric studies was designed as detailed in ref. [14b]. Voltammetric scans were referenced by addition of a small amount of ferrocene as internal standard at an appropriate time of the experiment. For referencing of the oxidized solution a small sample (ca. 3 mL) was transferred from the electrolysis cell to the voltammetric cell, the required amount of ferrocene added, and voltammetric traces were recorded. Higher electric currents could not be obtained in the CVs due to solubility and adsorption problems; b) R. F. Winter, F. M. Hornung, *Organometallics* **1999**, 18, 4005–4014.
- [15] For general information on the electrochemistry of ferrocenes, see a) P. Zanello in *Ferrocenes* (Eds.: A. Togni, T. Hayashi), VCH, Weinheim, **1995**; b) D. Astruc, *Electron Transfer and Radical Processes in Transition Metal Chemistry*, Wiley-VCH, Weinheim, **1995**.
- [16] Values at  $v = 0.2 \text{ V s}^{-1}$ . For the internal ferrocene standard, a peak potential difference  $\Delta E_p$  of 82 mV was obtained under these conditions.
- [17] P. D. Beer, P. A. Gale, G. Z. Chen, *J. Chem. Soc. Dalton Trans.* **1999**, 1897–1909.

## Li-Intercalated Oxometallobucanes

### Intercalation of Alkali Metal Cations into Layered Organotitanium Oxides\*\*

José Gracia, Avelino Martín, Miguel Mena,\*  
María del Carmen Morales-Varela, Josep-M. Poblet,  
and Cristina Santamaría

Dedicated to Professor Pascual Royo  
on the occasion of his 65th birthday

Species with a metallobucane structure constitute an interesting building block in inorganic solids, and considerable effort has been invested in selecting the composition and geometry of the precursor complexes to obtain specific characteristics and properties.<sup>[1]</sup> Some examples of the wide variety of inorganic materials whose structures are based on molecular cubane-like motifs are the molybdenum<sup>[2]</sup> and aluminum phosphates,<sup>[3]</sup>  $M_x\text{Mo}_y\text{P}_z\text{O}_w$  ( $M$  = metal cation), or various hydroxometalates  $[M_x\text{O}_y(\text{OH})_z]\text{L}$  ( $M$  = Ge, Ln,...).<sup>[4]</sup>

We have reported the formation and structure of the oxoheterometallobucanes  $[\{(\text{CO})_3\text{Mo}\}(\mu_3\text{-O})_3\{\text{Ti}_3(\eta^5\text{-C}_5\text{Me}_5)_3(\mu_3\text{-CR})\}]$  ( $R = \text{H}, \text{Me}$ )<sup>[5]</sup>, which were obtained from the preorganized organometallic oxides  $[\{\text{Ti}(\eta^5\text{-C}_5\text{Me}_5)(\mu\text{-O})\}_3(\mu_3\text{-CR})]$  ( $R = \text{H}$  (**1**),  $\text{Me}$  (**2**)).<sup>[6]</sup> Once we observed that the latter might be involved directly as macrocyclic tridentate ligands in encapsulation processes of different metals, we became interested in incorporating diverse metal complex fragments at the free vertex of the  $\mu_3$ -alkylidyne oxo derivatives to build up the corresponding oxoheterometallobucanes.

As part of these ongoing studies, here we present the intercalation of alkali metal ions into layered organometallic titanium oxides by treatment of the alkylidyne complex **1** with different alkali metal alkyl and amide reagents.

The one-pot reaction of the tripodal starting material **1** with MR ( $M = \text{Li}, R = \text{CH}_2\text{SiMe}_3, \text{CH}_2\text{CMe}_3, n\text{Bu}$ ;  $M = \text{Na}, R = n\text{Bu}$ ;  $M = \text{K}, R = n\text{Bu}, \text{CH}_2\text{Ph}$ ) in toluene/hexane at room temperature leads to the oxoheterometallobucanes **3–5** in good yields. These compounds can be also obtained by

[\*] Dr. M. Mena, Dr. A. Martín, M. d. C. Morales-Varela,  
Dr. C. Santamaría  
Departamento de Química Inorgánica  
Universidad de Alcalá, Campus Universitario  
28871 Alcalá de Henares-Madrid (Spain)  
Fax: (+34) 91-885-4683  
E-mail: miguel.mena@uah.es

J. Gracia, Prof. Dr. J.-M. Poblet  
Departament de Química Física i Inorgànica  
Universitat Rovira i Virgili  
Imperial Tarraco 1, 43005 Tarragona (Spain)

[\*\*] Financial support for this work was provided by the Ministerio de Ciencia y Tecnología (BQU2001-1499 and PB98-0916-CO2-02), Universidad de Alcalá (2002/010), and Generalitat de Catalunya (SGR01-00315). M.C.M.-V. thanks the Comunidad de Madrid for a doctoral fellowship.